Steel and Composite Structures, *Vol. 23, No. 1 (2017) 115-130*
DOI: https://doi.org/10.12989/scs.2017.23.1.115

Anchored blind bolted composite connection to a concrete filled steel tubular column

Hossein Agheshlui [*1], Helen Goldsworthy [1a], Emad Gad [2b] and Olivia Mirza [3c]

[1] *Department of Infrastructure Engineering, The University of Melbourne, Vic 3010, Australia*
[2] *Faculty of Engineering & Industrial Sciences, Swinburne University of Tech., Vic 3122, Australia*
[3] *School of Computing, Engineering & Mathematics, University of Western Sydney, NSW, 2751, Australia*

(*Received May 05, 2016, Revised December 14, 2016, Accepted December 15, 2016*)

Abstract. A new type of moment-resisting bolted connection was developed for use in composite steel- concrete construction to connect composite open section steel beams to concrete filled steel square tubular columns. The connection was made possible using anchored blind bolts along with two through bolts. It was designed to act compositely with the in-situ reinforced concrete slab to achieve an enhanced stiffness and strength. The developed connection was incorporated in the design of a medium rise (five storey) commercial building which was located in low to medium seismicity regions. The lateral load resisting system for the design building consisted of moment resisting frames in two directions. A major full scale test on a sub-assembly of a perimeter moment-resisting frame of the model building was conducted to study the system behaviour incorporating the proposed connection. The behaviour of the proposed connection and its interaction with the floor slab under cyclic loading representing the earthquake events with return periods of 500 years and 2500 years was investigated. The proposed connection was categorized as semi rigid for unbraced frames based on the classification method presented in Eurocode 3. Furthermore, the proposed connection, composite with the floor slab, successfully provided adequate lateral load resistance for the model building.

Keywords: Ajax anchored blind bolts; concrete filled steel hollow sections; composite steel-concrete connections; T-stub connections; moment-rotation behaviour; reinforced concrete slab on metal decking

1. Introduction

Structural hollow sections with or without concrete infill are used in the construction of low to medium rise building frames. Compared to concrete filled sections, construction using unfilled sections is significantly lighter. However, the unfilled sections have limited axial capacity and connections to them have low moment resistance due to the flexibility of the faces of tubular members. Concrete filled sections, on the other hand, have excellent axial capacity, ductility and rotation capacity (Bergmann *et al*. 1995). Extensive studies have been conducted on the behaviour of these sections as columns filled with normal and high strength concrete (Chung *et al*. 2013, Aslani *et al*. 2015, Qu *et al*. 2015). Construction using these sections has been well established. The concrete pour can be done using the top filling or bottom pressure filling methods and the concrete infill does not normally require curing since it is protected and cannot dry out (Hicks and Newman 2002). Filling the steel tubes with concrete is also advantageous in reducing the flexibility of bolted connections to them (France *et al*. 1999).

Despite the merits of CFSHS columns, their use is not as widespread as it could potentially be, because practical moment resisting bolted connections to these sections are not well developed. Blind bolts, such as Ajax Oneside, Flowdrill and Hollo-Bolt which can be installed by having access to only one side of a connection, have been used for connections between open section beams and CFSHS columns (France *et al*. 1999, Gardner and Goldsworthy 2005, Loh *et al*. 2006, Wang *et al*. 2009, Liu *et al*. 2014). To achieve an enhanced moment resisting behaviour of such blind bolted connections, extensions that are embedded or anchored within the infill concrete have been added to blind bolts (Tizani and Ridley-Ellis 2003, Gardner and Goldsworthy 2005, Yao *et al*. 2008, Pitrakkos and Tizani 2015). Studies on the behaviour of Ajax Oneside with different types of welded extensions (Gardner and Goldsworthy 2005, Yao *et al*. 2008), showed a significant increase in the bolt capacity and stiffness which in turn resulted in a higher capacity and stiffness of bolted connections. Tizani *et al*. (2003) introduced the idea of adding a straight extension with a head at its end to commercial Hollo-Bolts, referred to as the Extended Hollo-Bolt (EHB). They concluded that EHB has improved stiffness characteristics compared with the standard Hollo-Bolt. Flush endplate and extended endplate connections using EHBs were tested (Tizani *et al*. 2013a) and were categorized as semi-rigid connections with an evident

*Corresponding author, Research Fellow,
E-mail: hossein.agheshlui@unimelb.edu.au
[a] Associate Professor, E-mail: helenmg@unimelb.edu.au
[b] Professor, E-mail: EGad@swin.edu.au
[c] Senior Lecturer, E-mail: o.mirza@uws.edu.au

ISSN: 1229-9367 (Print), 1598-6233 (Online)

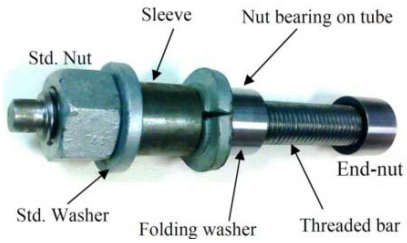

Fig. 1 Ajax anchored blind bolt

enhancement in the moment-rotation behaviour compared to the use of Hollo-bolts. The cyclic behaviour of endplate connections using EHBs was also investigated (Tizani *et al*. 2013b) and it was shown that they provided stable hysteretic behaviour with an appropriate level of strength and stiffness, where strength was comparable to that of standard bolt-and-nut fasteners. Yao *et al*. (2008) studied the tensile behaviour of T-stubs connected to concrete filled circular and square hollow sections using Ajax Oneside with welded cogged extensions. They showed that using the cogged extension the behaviour of the T-stub connections in tension was improved and excessive localized deformation of the tube walls was avoided (Yao *et al*. 2008). In the case of square concrete filled sections, the connection was categorized as rigid for braced frames. To avoid a welded extension and to provide a simpler installation of bolts, Yao *et al*. (2011) used a straight extension with a head at its end, referred to as "Ajax anchored blind bolt" (Fig. 1). The tensile behaviour these bolts, as individuals and groups used in CFSHS members, was studied in detail (Agheshlui 2014) and it was shown that for anchored bolts installed close to the side walls of a CFSHS, concrete struts develop which provide a significant stiffness with a tensile capacity of the breaking load of the threaded bar. A simple theoretical model was also developed to provide a bilinear estimate of the tensile behaviour of such anchored blind bolts (Agheshlui 2014).

In this study, a new type of moment-resisting connection between open section beams and a CFSHS column using Ajax anchored blind bolts was proposed and tested. The aim was to develop a lateral load resisting system for medium-rise (4 to 7 stories (HAZUS MR4 2003)) commercial buildings which use CFSHS columns in low to moderate seismicity regions such as Australia. Earthquakes in these regions, also referred to as intraplate areas, are less common compared to high seismicity regions. A five storey commercial building with moment-resisting frames was designed as a case study. The steel beams in these frames were composite with the floor slab with spans of 12.6 m for the internal frames and 8.4 m for the perimeter moment resisting frames. The only lateral load resisting system provided for the building frame was the moment-resisting frames with anchored blind bolted connections. The connections were acting compositely with the floor slab. Guidelines for the design of composite connections have already been developed (SCI P213 1998); however, connections to CFSHS columns that are composite with the floor slab have not been investigated. A sub-assembly of the perimeter frame including the effective width of the floor slab was selected for a full-scale sub-assembly test. The specimen was tested under practical gravity loads and lateral loads that represented two different earthquake levels. The test set-up, results and the connection behaviour as part of a composite structural system are presented here.

2. Case study

A structural frame for a medium rise commercial building has been designed in order to provide a realistic estimate of the section sizes and loading conditions for the sub-assembly test. The frame was a 5 storey frame with storey height of 4m at the ground floor and 3.5m for the rest of the floors and it did not include a transfer structure. The plan layout of the building frame, identical throughout the building, is shown in Fig. 2. The perimeter frames were designed to be moment resisting. To reduce the section sizes of the interior primary beams in the Y direction (see Fig. 1), the interior frames in that direction were also selected to be moment resisting. The loads applied to the model building due to gravity included an estimated permanent load of 5 kPa (a dead load of 4 kPa and a superimposed dead load of 1 kPa) and an imposed (live) load of 3 kPa for floors and 1.5 kPa for the roof. External curtain walls with a self-weight load per unit area of 2 kPa were considered on perimeter frames. Earthquake loads were determined in accordance with the Australian Standard, AS 1170.4 (2007). Considering that the importance level of the case study building was 2 in accordance with Australian/New Zealand Standard AS/NZS 1170.0 (2002), it was required to design the building for an earthquake with probability of exceedance of 1/500. However, as argued in the commentary to AS 1170.4 (2007), designing for a return period of 2500 years leads to a risk of collapse that is comparable to that in high seismicity regions. Hence, the building studied here was designed considering two different performance objectives of life safety and collapse prevention under earthquakes with return periods of 500 and 2500 years, respectively. The building was assumed to be located in a low to moderate seismicity area on a class D soil as defined by AS 1170.4 (2007). The seismic forces were applied in two perpendicular directions at the mass centre of each floor considering a 10% accidental eccentricity in accordance with AS 1170.4 (2007). The design against the wind lateral load was conducted in accordance with AS 1170.2 (2011). A 3D analysis of the model building adopting a non-linear global analysis method was conducted using ETABS. The storey drift of 1.5% was controlled under the design level (500 year return period) earthquake as required in AS 1170.4 (2007) and a maximum of 0.2% storey drift was checked under the serviceability wind load as required by AS 1170.2 (2011). The design of the model building was performed in accordance with EN 1994-1-1 (2004), since Australian Standards for the design of composite buildings were not fully published at the time of this research. The required section for the gravity design of interior columns supporting 12.6m long spans (see Fig. 2) was C350 grade SHS 400×400×12.5 filled with 50 MPa concrete. The column

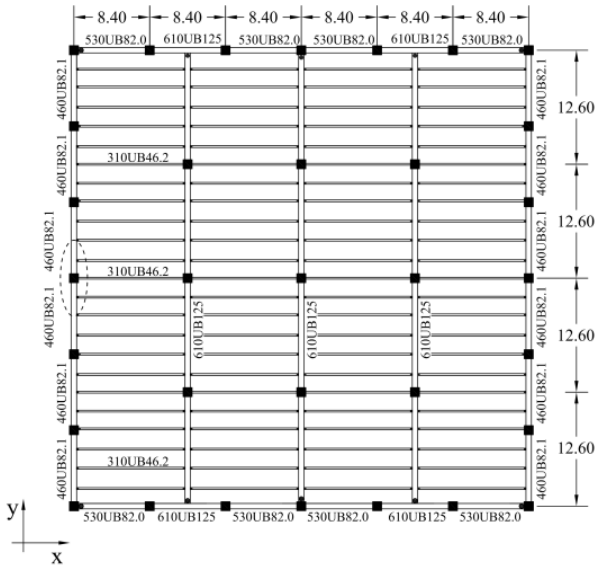

Fig. 2 Floor plan of the model building. Beam ends with a dot are not moment resisting

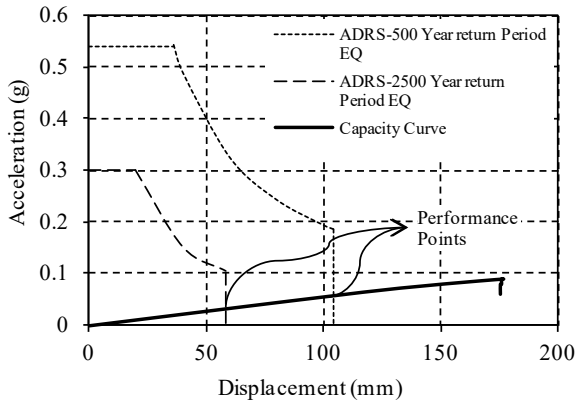

Fig. 3 Performance points of the building for 500 and 2500 year return period earthquakes

design was conducted in accordance with EN 1994-1-1 (2004) for concrete filled rectangular hollow steel sections. Axial load of such columns was about 8000kN with a utilization factor of about 0.75. For consistency, the same section was used for all other columns. Beams with different sections ranging from 310UB46.2 to 610UB125 were used composite with an in situ 140 mm thick concrete slab. Beam sections are shown in Fig. 2. The floor slab was composite with steel sheeting (Sayers *et al*. 2009) and was designed in accordance with EN 1994-1-1 (2004). Shear studs were designed to provide a full shear transfer between the slab and the steel beams.

2.1 Design approach for the 2500 year return period event

The lateral load due to the 2500 year return period earthquake was determined based on AS 1170.4 (2007). The model building was designed for the 500 year return period earthquake. Then its displacement capacity was controlled for the 2500 year return period earthquake. To provide the required displacement capacity, beam-column connections were designed to become plastic at a particular moment. This was because, considering the strength hierarchy, columns needed to remain in elastic range. Developing plastic hinges in beams was not practical and desirable since Australian practice demands large beam sections; also residual deformations in beams are not generally repairable. Hence, connections were selected to act as fuses by exhibiting nonlinear behaviour at a defined load level corresponding to the maximum design moment which occurred under the G+0.3Q+EQ500 load case, where G, Q, and EQ500 refer to permanent loads, imposed loads, and earthquake action with a return period of 500 years, respectively. The plastic behaviour was designed to initiate at T-flanges before the maximum bolt load reached 60% of the capacity of the anchored blind bolts to avoid significant deterioration of their stiffness and their eventual brittle failure. Agheshlui *et al*. (2016) showed that Ajax anchored blind bolts located close to the side walls of a concrete filled hollow section (as they have been used in this research) reach the ultimate capacity of the equivalent structural bolts (M24 8.8).

Using a capacity spectrum (ADRS diagram) method developed by Lam *et al*. (Lam and Wilson 2004) for intraplate earthquakes, such as Australia, it was concluded that the structure would have sufficient displacement capacity to withstand the 2500 year return period earthquake. The capacity curve of the structure (nonlinear push-over curve divided by the dynamic mass of the structure) was intercepted with the Acceleration-Displacement Response Spectra (ADRS) curves for earthquakes with return periods of 500 and 2500 years (AS 1170.4 2007) to obtain performance points of the structure for the corresponding earthquake events (Fig. 3). The performance points determined the displacement demands of the structure for the mentioned events which were less than the displacement capacity of the structure presented by the capacity curve.

2.2 Proposed connections

The design of the proposed connections was governed by the load combination that produced the largest connection moments (G+0.3Q+EQ500). The proposed anchored blind bolted connections used T-stubs at the top and the bottom of the beams as illustrated in Fig. 4. Each T-stub was connected to the CFSHS column using four anchored blind bolts and a through bolt. The through bolts were used to further enhance the connection behaviour. They were isolated from the infill concrete using steel sleeves. Through bolts were only used in the middle of the column section (see Fig. 4) where the use of anchored blind bolts was shown to be not efficient (Agheshlui 2014). The use of through bolts in connections to CFSHS columns has been investigated before (Ricles *et al*. 2004) and it has been shown that their use can provide cyclic joint stiffness and strength. In the proposed connections, the top connection was composite with the reinforced concrete slab which provided a greater moment capacity and stiffness. The connection at the bottom only relied on the anchored blind

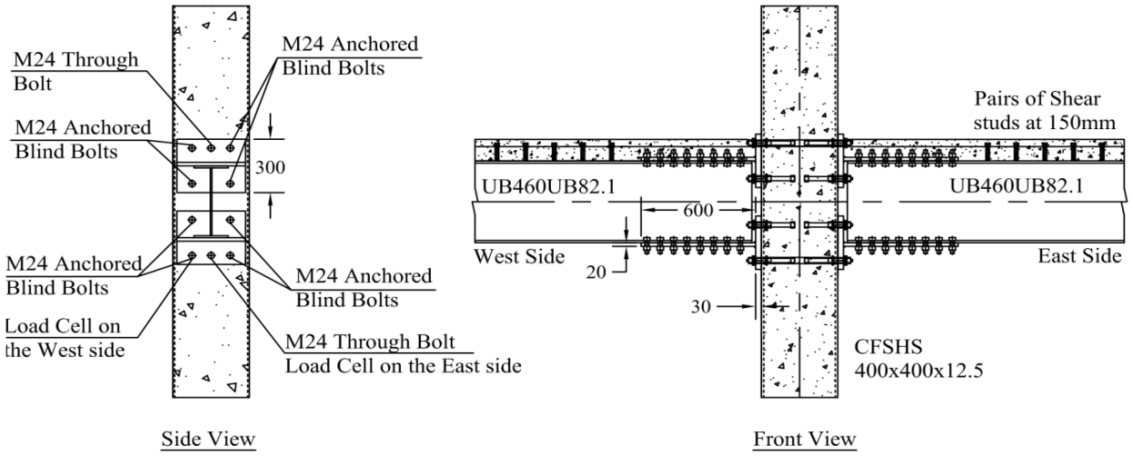

Fig. 4 Proposed anchored blind bolted connection for the sub-assembly test

Table 1 Material used in the sub-assembly test

Material	Mechanical properties
SHS Column	f_y = 378 MPa; f_u = 490 MPa
I-Beam flange	f_y = 353 MPa; f_u = 507 MPa
I-Beam web	f_y = 354 MPa; f_u = 523 MPa
T-flange	f_y = 373 MPa; f_u = 493 MPa
T-stem	f_y = 366 MPa; f_u = 501 MPa
Anchored blind bolts	f_y = 710 MPa; f_u = 860 MPa
Through bolts	f_y = 745 MPa; f_u = 930 MPa
Concrete- Column infill, slab	Average of four cylinders at the test day: 46 MPa

bolts and one through bolt. The difference in the behaviours of the top and bottom connections could clearly demonstrate the influence of the composite action between the T-stub connection and the floor slab in the overall connection behaviour. For the rest of the connections in the model building, blind bolts with no extension were used and the slab did not have extra reinforcement to provide a considerable contribution to the connection behaviour. These connections were expected to act as pin connections.

3. Test set-up

The perimeter frames were the main source of resistance against lateral loads. Hence, the connection selected to be tested was chosen from a perimeter frame in the load carrying direction. The selected sub-assembly is shown in Fig. 2. The ideal column height for the sub-assembly specimen was half of its height from the top and the bottom floors which corresponded to the contraflexure points of bending moment diagrams under lateral loads. However, due to the laboratory limitations, the column height was limited to 2.2 m. However, this was not assumed to be an issue since the moment-rotation behaviour of CFSHS members is well known (EN 1994-1-1 2004) and it was not the focus of the study. The beam lengths were half their length from each side (4.2 m). The test set-up for the sub-

Fig. 5 Sub-assembly specimen

assembly test is depicted in Fig. 5. The full-scale specimen was fabricated and tested at The University of Western Sydney. The mechanical properties of materials used in the test are presented in Table 1. The concrete strength, tensile properties of steel members and the tensile behaviour of bolts were determined by cylinder tests, coupon tests and tensile tests, respectively. The concrete slab width was equal to the effective width of the slab over the selected beams of the model building in accordance with EN 1994-1-1 (2004) (≈ 0.1× the beam span). Slab reinforcement was of grade D500N (normal ductility class) in accordance with AS/NZS 4671 (2001) and the grade of shear studs was 6.8 in accordance with AS 4291.1 (2000). All the bolts used in the specimen were 8.8 in accordance with AS 4100 (1998).

3.1 Loading regime

The sub-assembly specimen was loaded by the critical design load combination, i.e., G+0.3Q+ EQ500, which was determined using a 3D analysis of the building frame. The focus was on replicating the bending moment diagram at the connections and on the beams close to the beam-column joint in a simple but effective manner (Fig. 6). Gravity loads of 150 kN were applied on the beams at 1.68 m (0.2L = 0.2 × 8.4) away from the centreline of the column to produce

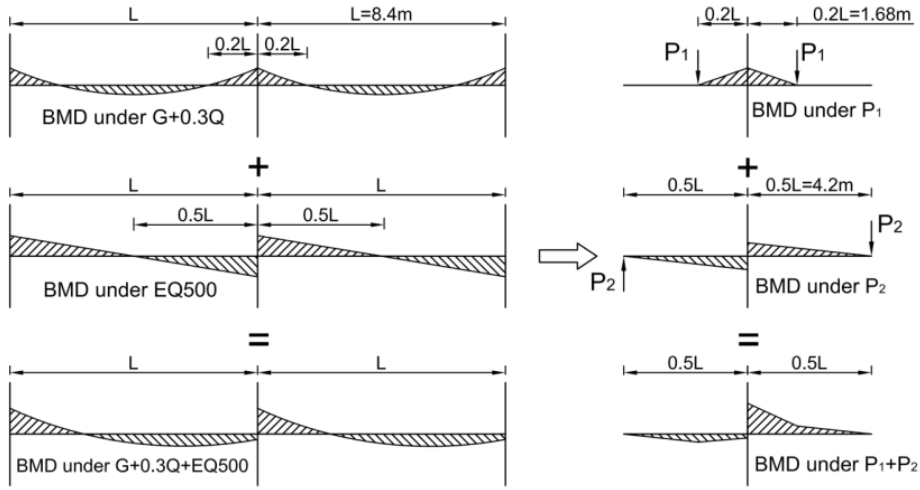

Fig. 6 Bending Moment Diagram (BMD) in the sub-assembly test

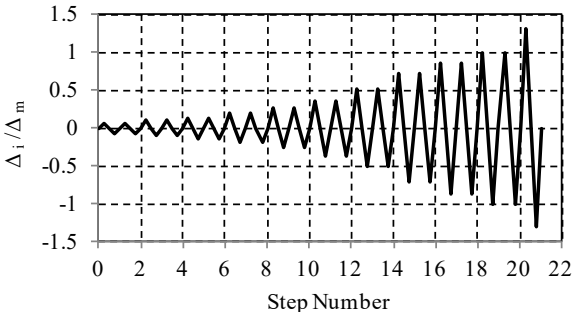

Fig. 7 Load regime designed for the sub-assembly test according to FEMA-461

the connection moment due to gravity loads. Also, beam end loads were applied as equal and opposite displacements at beam ends to replicate the bending moments caused by lateral loads. An axial load of 1900 kN was applied to the column using a hydraulic jack. This represented the axial load on the selected column from the design building under the design load case mentioned previously.

Five loading frames were employed to apply the required loads to the specimen. These included the central frame to apply the column gravity load; two frames to apply the gravity loads on beams; and two frames to exert cyclic displacements at the beam ends. The column was fixed at the bottom by relying on the friction force between the column and the strong floor and at the top by the friction between the column and the loading plate beneath the hydraulic jack used to axially load the column. The friction force produced by the 1900 kN axial force provided the stability of the specimen by a safety factor of two relative to the estimated horizontal reaction. Fly braces were used to inhibit the lateral torsional buckling of beams. All the bolts used in the specimen, including the anchored blind bolts and the through bolts, were fully tensioned prior to pouring the infill concrete.

The loading protocol developed by FEMA 461 (2007), was selected for this test since it provides an adequate number of steps and cycles in the linear and nonlinear regions. The loading regime, shown in Fig. 7, uses a targeted maximum deformation amplitude, Δ_m = 110 mm, and a targeted smallest deformation amplitude, Δ_0 = 7 mm, as reference values, and a predetermined number of increments, n = 10, to determine the loading history. Each step was executed twice and had an increase of 40% compared to the previous step. If the specimen had not failed before the 10th step, the 11th step with a 30% increment compared to the 10th step was to be applied (FEMA 461 2007). In total, 20 cycles were designed to be applied before the failure. The plan was to load the specimen up to the failure load with displacements applied in opposite directions at the ends of the beams, and then to apply increasing displacements in the same direction at both ends, first upwards and then downwards in order to determine the maximum positive and negative moment capacities of the connections.

3.2 Instrumentation

23 LPs (Linear Potentiometer) were employed to measure displacements at different locations on the specimen as illustrated in Fig. 8. These were used to measure the absolute displacements of the column and the beams, and the relative displacements of the T-stubs and the bolts at different locations. Also, 26 strain gauges were mounted on the column, beams, T-stubs and slab reinforcement. Fig. 9 shows the strain gauges mounted on the reinforcing bars. Two load cells for measuring the bolt loads of an anchored blind bolt and the through bolt at the bottom connection were used. They were installed on bolts between T-flanges and nuts. Hobson squirter DTI washers were used under the nuts for all the bolts to ensure that the required pre-tension force was applied to them. In accordance with AS 4100 (1998), a minimum bolt tension of 210 kN needed to be applied to the M24 bolts. This was equivalent to 70% of the ultimate strength of the tested bolts. Orange silicon was squirted out when the specific tension in the bolt was achieved. The squirter washers were calibrated using hollow load cells in previous bolt tensile tests (Agheshlui 2014).

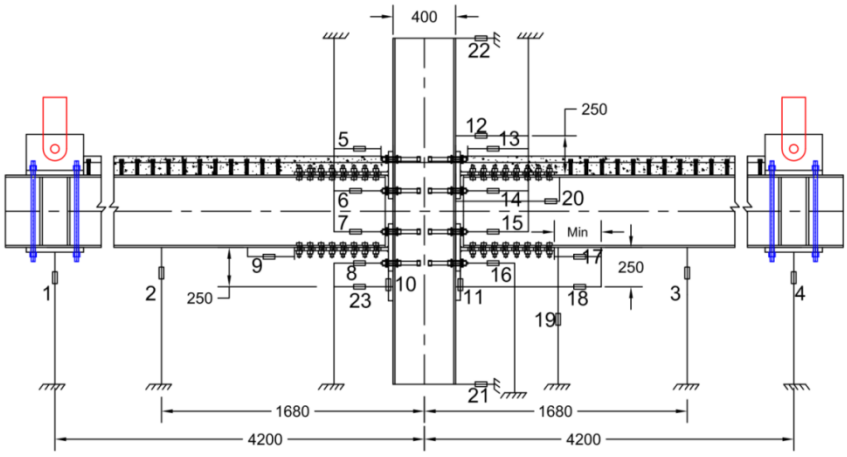

Fig. 8 LPs used on the specimen

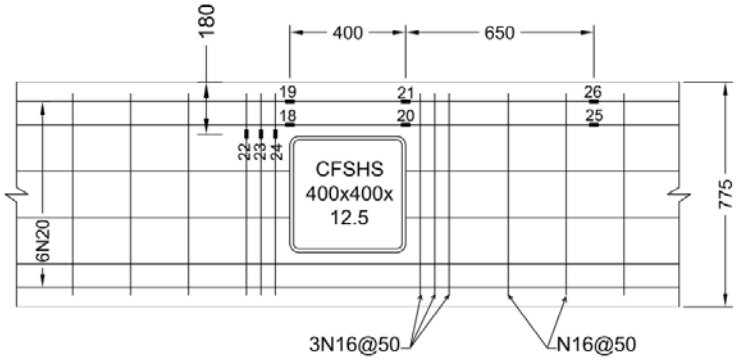

Fig. 9 Strain gauges mounted on the reinforcement

4. Results

The readings conducted on both sides of the specimen were similar due to the symmetry of the specimen and loading. In cases that the results were different on the sides, the results for both sides are presented.

4.1 Sub-assembly behaviour under Gravity loads

The moment-rotation curves of the connections were obtained using three different methods. These included the rotation calculation based on beam end deflection, horizontal displacements of T-stubs and vertical displacements of the connection area. The connection moment-rotation curves are shown in Fig. 10(a). The measured pullout displacements of the anchored blind bolts were almost zero (less than 0.05 mm). This was because the bolts were fully tensioned (pre-tensioned to the bolt's proof load) and the maximum load applied to each bolt (around 100 kN calculated based on connection moment) was less than the pretension load existing in them. Prior to the test, it was assumed that no slip (relative displacement between structural members) would occur between the bottom beam flanges and the bottom T-stems until the slip load of approximately 820 kN was reached (16 fully tensioned M24 structural bolts were used). The load applied to the T-stub versus the beam slip is shown in Fig. 10(b) for the connections on both sides of the column. Although the amount of slip was very small, there was a linear trend in the load-slip relationship and the slip started from an early stage. This differs from the traditional serviceability design assumption in which it is assumed that there is no slip before reaching the slip load. Further detailed investigations are currently being conducted to determine the reason for this behaviour and to prevent this slip from occurring.

4.2 Cyclic loading of the specimen

With the gravity loads in place, cyclic loads were applied at the beam ends as simultaneous opposite displacements. The moment-rotation curve for the whole loading history is shown in Fig. 11(a). The cyclic moment-rotation curve started and evolved around an initial moment of -222 kNm produced by the gravity loads. In later stages, the negative gravity moment was overcome by the positive moment due to the load at the beam end. The test was stopped after the first cycle of the 11th step (21 cycles) when it was believed that repeating the cycle or conducting a larger load step might compromise the stability of the specimen.

A plateau was observed in the middle part of the moment-rotation curve which reduced the connection stiffness significantly. Three potential phenomena including the slip of the beam on the bottom T-stub, the slip between the beam and the top T-stub, and the crack opening and closure in the slab in the connection region were considered

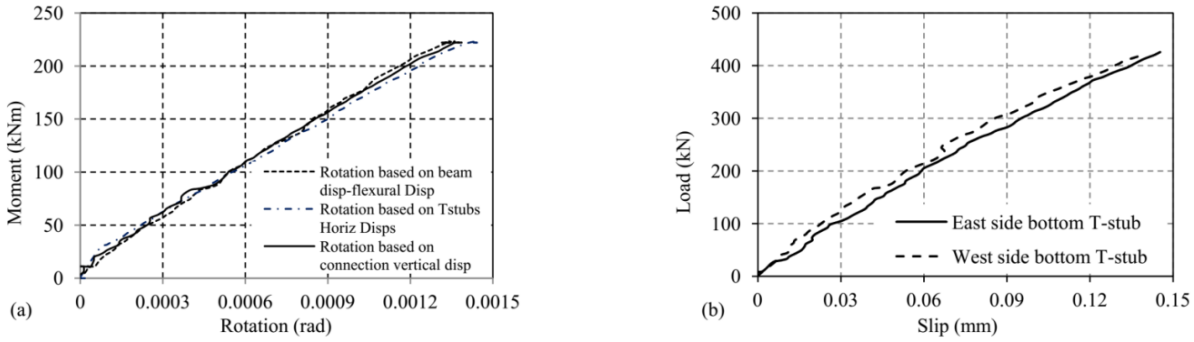

(a) (b)

Fig. 10 (a) Moment vs. rotation; (b) T-stub load vs. T-stub slip under gravity loads

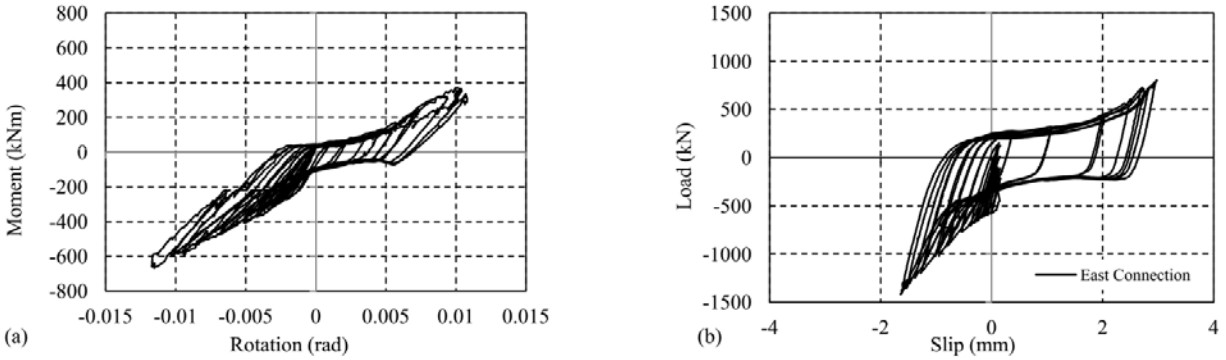

(a) (b)

Fig. 11 (a) Cyclic moment-rotation behaviour of composite anchored blind bolted connections; (b) bottom T-stub load vs. slip displacement

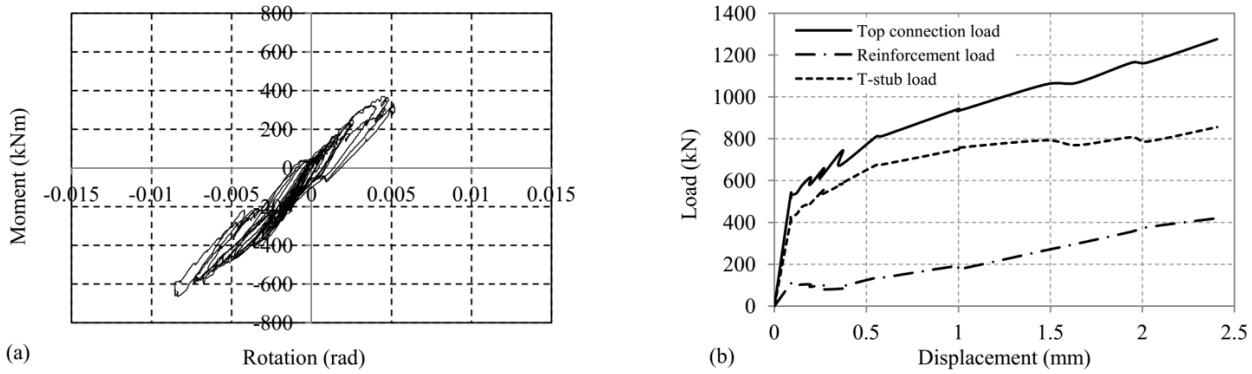

(a) (b)

Fig. 12 (a) Moment-rotation curve ignoring the slip on the bottom T-stub; (b) Load distribution between the top T-stub and slab reinforcement

as potential causes. The amount of slip at the top T-stub was insignificant because the concrete slab, which was connected to the steel beam and the top T-stub, minimized relative displacement between the beam flange and the top T-flange. The cracks in the slab in this stage were not sufficiently developed to make a significant influence on the moment-rotation behaviour. Therefore, the plateau was expected to be a result of the beam slip on the bottom T-stub. As shown in Fig. 11(b), the slip curve has a plateau similar to the one observed in the moment-rotation curve.

Fig. 12(a) depicts the cyclic behaviour of the connection after deducting the slip effect from the total rotation of the connection. As can be seen, a substantial change is observed in the cyclic behaviour after removing the slip effect in that the pronounced flat area in the hysteresis curve is no longer is present. The remaining small slip was due to the crack opening and closure in the slab and the slip at the top T-stub. These effects are inevitable and they have to be

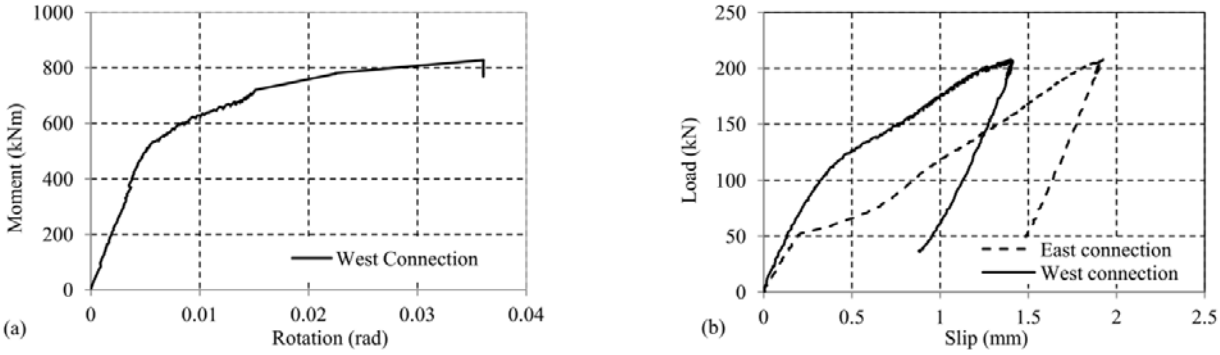

(a) (b)

Fig. 13 (a) moment-rotation behaviour of the connections under a monotonic positive moment; (b) beam end load vs. slip at the bottom connections

considered in the connection behaviour. However, the slip at the bottom T-stub could be inhibited or mitigated by providing more frictional bolts or increasing the roughness of the shear surfaces. Hence, the effect of slip on the bottom T-stubs is not included in subsequent sections of this paper.

The strain at reinforcing bars at the face of the column measured by, SGs 18, 19, and 21 in Fig. 9, were used to calculate the load carried by the reinforcement. All three strain gauges recorded a similar linear increase due to the increasing tensile load applied at the connection. This shows the direct contribution of the reinforcement in the moment carrying capacity of the composite connection. Substantial forces were developed although the reinforcement did not yield at the column face during the cyclic loading. The rest of the tensile load at the top connection was assumed to be carried by the top T-stub. Fig. 12(b) illustrates the load distribution of the top connection between the reinforcement and the T-stub versus the net outward displacement of the top T-stub (measured by LP20 minus the displacement due to the column flexural rotation) during the cyclic loading. In these curves, the envelopes of the cyclic curves are shown to provide a clearer presentation of the behaviour. As shown, the stiffness of the T-stub was significantly larger than the stiffness of the slab reinforcement. Consequently, most of the tensile load at the connection was taken by the T-stub, especially in the initial stages.

Strains measured at 650 mm away from the face of the column (SG25 and SG26) had a similar turned to the ones observed at the face of the column. However, these strains were smaller, due to the transfer of the rebar force to the concrete via the bond effect within that length. The ratio of the strains at 650 mm away from the face of the column to the ones at the face of the column was inversely related to the moment at the connection.

Other strains measured included those from strain gauges mounted on the tube face. These indicated that the hoop stress in the steel tube due to the axial column load was very small. Strains measured on the bottom T-flange showed that it yielded in the final steps of cyclic loading at the connection line of the T-flange to the T-stem. The yielding occurred at a higher load than expected which created large forces in the bolts. This is discussed further in Section 4.5.1.

4.3 Sub-assembly test results for loading beam ends upward

Both beam ends were loaded upward after completing the cyclic loading of the specimen. The gravity loads on the beams were removed. The moment-rotation curve of the connection, which is dominated by the behaviour of the bottom T-stub, is shown in Fig. 13(a). Assuming a bilinear behaviour, at 2/3 of the yield moment, the secant stiffness is 110,000 kNm/rad which is as the same as the stiffness observed during the cyclic loading. Since the stiffness of the connection depended to a large extent on the stiffness of the anchored blind bolts, it could be concluded that the deterioration of the anchorage behaviour was insignificant after applying 21 cycles of loads. The T-stub tensile load versus the slip at the bottom connections is depicted in Fig. 13(b). The significant difference between the two curves could be related to the different initial conditions at the two sides of the specimen due to the previously conducted cyclic loading. The maximum amount of slip was about 1.8 mm.

The strain at the middle of the T-flange just above and below the T-stem versus T-stub load of the top and bottom T-stubs are shown in Fig. 14(a). In the bottom T-stub, the strains above (SG12) and below (SG13) the T-stem were similar and they both showed that the T-flange yielded when the tension load applied to the connection due to positive moments reached about 900kN. This suggested a symmetrical behaviour for the bottom T-flange with minimal tilting. The top T-stub was under compression and its strain was very small (SG15).

4.4 Sub-assembly test results for loading beam ends downward

In the final load case both beam ends were pushed downward to exert negative moments on the connections. The aim was to determine the ultimate capacity of the composite connections. The moment-rotation curve of the connection is shown in Fig. 14(b) which includes an initial soft region. This was because, prior to this load step, the beams were pulled upward, which resulted in yielding of the bottom T-flanges. Hence, before the bottom connections could provide a reasonable compression resistance, they needed to be flattened. The corrected moment-rotation

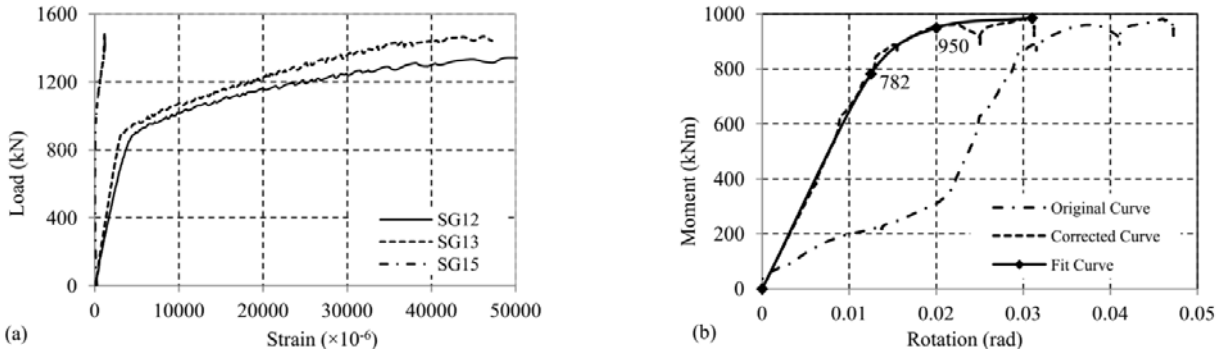

(a) (b)

Fig. 14 (a) Strain at mid-thickness of T-flange vs. the load applied to T-stubs; (b) Moment-rotation behaviour of the connections under negative moments

Table 2 Experimental behaviour of anchored blind bolted connections

Connection type	Elastic stiffness (kNm/rad)	M_y (kNm)	M_u (kNm)
T-stub-Slab	196,000	780	983
T-stub	110,000	500	832

curve, without the initial flat region, is also shown in Fig. 14(b). In Fig. 14(b), a fitted curve illustrates the yield moment of the proposed composite anchored blind bolts.

The concrete slab in the connection region was extremely damaged during this load step. Hence, the strains in the reinforcement were not measured accurately up to the ultimate load. However, up to about half of the ultimate load, the transverse bars did not yield. The longitudinal reinforcement had yielded at this stage. The strains in the longitudinal reinforcement at 650 mm away from the column were significantly lower than the strains at the face of the column. This suggested strain localization at regions closer to the column which eventually resulted in yielding of the reinforcement at the face of the column.

Various other phenomena are noteworthy. The top T-stub eventually yielded at the T-stem to T-flange connection at close to the ultimate load, despite the restraining effect of the concrete slab on the T-flange. The maximum shear displacement of the beams measured by LPs 10 and 11 was less than 1mm, under ultimate load. This was due to the reduced clearance in the bolt holes of the anchored blind bolts due to the use of shear sleeves which allowed an effective shear transfer.

4.5 Discussion

Table 2 presents the experimental values for the elastic stiffness, $k_{elastic}$, yield moment, M_y, and ultimate moment, M_u, of the composite and non-composite anchored blind bolted connections, shown respectively at the top and bottom of the beam in Fig. 4.

4.5.1 Connection capacity

In the design of the T-stub connections, the intention was to limit the tensile load of the anchored blind bolts to 60% of their capacity. It was assumed that due to the difference in the lever arms of the bolt lines of a T-stub from the pivot line (see Fig. 15), the loads taken by the bolt lines would be different under a certain rotation angle. Also, it was assumed that the load taken by a through bolt will be less than the load taken by an individual anchored blind bolt from the same bolt group due to its lower stiffness. Stiffness estimations for bolts are presented in the next section. However, the readings of the bolt load cells and the high moment capacity of the connections showed that all the five bolts used in a T-stub connection reached their ultimate capacity. Bolt loads in an anchored blind bolt and a through bolt used at bottom connections are presented in Fig. 16, when the beam ends were loaded upward and the bolts carried a monotonic tensile load. As shown, both types of bolts have reached their ultimate capacity based on the ultimate tensile stresses given in Table 1. The difference in the ultimate bolt loads was due to the difference in the materials used for the through bolt and the anchored blind bolt.

The equal loads of the bolt lines of a T-stub can be explained considering Fig. 15, which shows the possible scenarios for the deformed shape of a T-stub. The deformed shape of the T-flange and the possible resulting prying forces are not the focus of the discussion here and are not considered in this figure. The deformed shape of the T-stub depends on the relative stiffness of the T-stem and the T-flange. The two extreme cases of the possible deformed shapes are shown in Figs. 15(b), (c). In Fig. 15(b), the T-flange undergoes the same rotation as the T-stem which can occur if the T-stem is relatively stiff compared to the T-flange. In the other extreme case, shown in Fig. 15(c), the T-flange remains vertical while the T-stem bends. This may occur if the T-stem is relatively flexible compared to the T-flange. Considering the thickness of the T-flange and the T-stem, the deformed shape was similar to Fig. 15(c). Hence, the bolt lines of the bottom T-stub carried almost the same amount of load. Fig. 17 shows the deformed shape of the bottom T-stub under the ultimate positive moment in which the T-stem rotation was not transferred to the T-flange. Prying forces were not expected based on the T-flange design. This was later confirmed by the measurements of the bolt load cells which matched well with the estimated loads based on the connection moments.

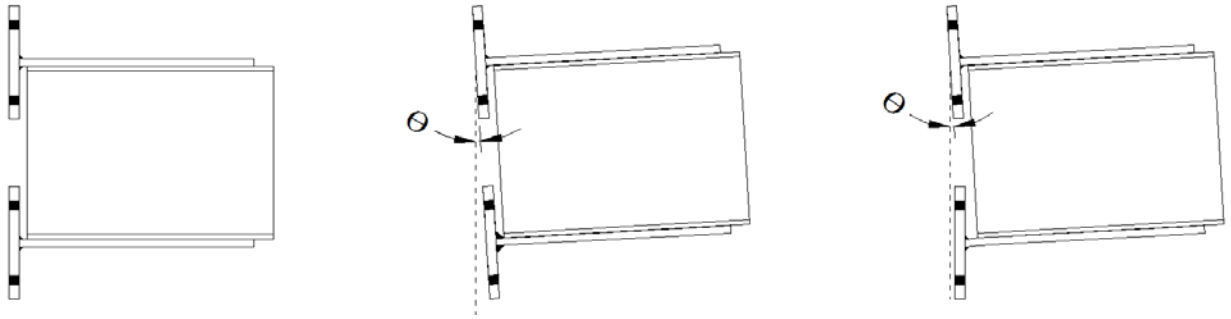

(a) Undeformed shape (b) Rigid connection between T-stem and T-flange (c) Pin connection between T-stem and T-flange

Fig. 15 Deformed shape of a T-stub depending on the T-stem to T-flange connection

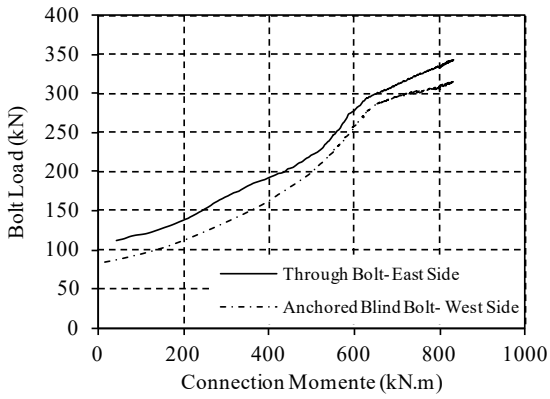

Fig. 16 Bolt loads measured by load-cells at the bottom connections

Fig. 17 Deformed shape of the T-flange at the ultimate load

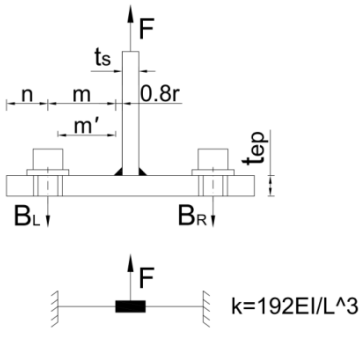

Fig. 18 Double curvature deformation of the T-flange

With regard to the load carried by through bolts, despite its lower stiffness compared to the anchored blind bolts, the ultimate tensile capacity of the bolt was reached. This was justifiable considering the strain capacity of the adjacent anchored blind bolts which resulted in the increase of the through bolt's load up to the ultimate load, while the adjacent anchored blind bolts were undergoing plastic deformations.

The ultimate strength of the connection was governed by the ultimate tensile capacity of five 8.8 M24 bolts (= 1485 kN (FEMA 461 2007)). Having the moment capacity of 832 kNm and the total tensile load of 1485 kN for the bottom connection, the lever arm of the connection was found to be 0.56 m which is the distance from the mid-thickness of the bottom T-stem to 2/3rd of the height of the concrete slab. Furthermore, the yield load obtained for the bottom T-stubs suggested a double curvature shape for the T-flanges. This was due to the clamping load applied at the bolt lines. Fig. 18 shows a T-stub under tensile load (based on (AS 4100 1998)) and a simplified fixed end beam model for it. The fixed ends reflect the clamping force applied at the bolt lines due to the bolt pretension. The estimated yield moment based on this simplified model is 504 kNm which is in excellent agreement with the experimental yield capacity of the T-stub. This shows that the fully-tensioned bolts provided adequate fixity at the bolt lines, which had a substantial influence on the strength and stiffness of the T-stubs as suggested in the literature (Faella *et al*. 1998).

Under negative moments, the lever arm was calculated to be from the centroid of the tension force (reinforcement and the bolts) to the centre of the compression force (mid-thickness of the bottom T-stem). Assuming that the reinforcement yielded when the T-flange started yielding, the lever arm was found to be at 0.56 m above the mid-thickness of the bottom T-stem. Therefore, the yield moment of the top connection (composite with the reinforced slab) was estimated to be 780 kNm which was in good agreement with the experimental result of 782 kNm (Fig. 14).

4.5.2 Connection stiffness

For estimation of the connection stiffness a component model was used. For the bottom connection, the stiffness of the T-flange, T-stem, and the anchored blind bolts (including the tube face deformation) needed to be

considered. Based on the simplified model shown in Fig. 18, the stiffness of the T-flange can be estimated using Eq. (1). The basis for Eqs. (1) to (3) can be found in (Hibbeler 2008).

$$K_{T-flange} = 192E_{tf}I_{tf}/{L_{tf}}^3 \quad (1)$$

Where E_{tf} is the elastic modulus of the T-flange; I_{tf} is the second moment of area of the T-flange section; L_{tf} is the distance between the bolt lines minus a bolt diameter (half of the bolt diameter from each side). Substituting the parameters in Eq. (1), the stiffness of the T-flange was found to be 3300 kN/mm.

The axial stiffness of the T-stem was calculated to be 2360 kN/mm using Eq. (2)

$$K_{TS-A} = E_{ts}A_{ts}/L_{ts} \quad (2)$$

In Eq. (2), E_{ts} is the elastic modulus of the T-stem; A_{ts} is the sectional area of the T-stem and L_{ts} is the length of the T-stem up to the bolt line farthest to the column. As discussed in Section 4.5.1, the T-stem bends so that its deformation is compatible with the beam's deformation. Therefore, the flexural stiffness of the T-stem also needed to be considered in the component model. The flexural stiffness of the T-stem has been estimated using Equation (3) in which I_{ts} is the second moment of area of the T-stem section. By substitution of the corresponding values into Eq. (3), the flexural stiffness of the T-stem is calculated to be 634 kN/mm

$$K_{TS-F} = 3E_{ts}I_{ts}/L_{ts}^3 \quad (3)$$

To calculate the stiffness of the bolt group, the stiffness of the through bolt and anchored blind bolts need to be estimated. The axial stiffness of the through bolt was calculated to be 154 kN/mm using Eq. (4).

$$K_{TB} = E_{TB}A_{TB}/L_{TB} \quad (4)$$

where E_{TB} , A_{TB} , and L_{TB} are the elastic modulus, tensile stress area and the elongation length of the through bolt, respectively. The stiffness of the group of four anchored blind bolts was estimated using Eq. (5) which was developed by Agheshlui *et al*. (2015) for similar groups of anchored blind bolts (Agheshlui, Goldsworthy *et al*. 2015).

$$K_{ABB} = 2 \times \left[1/\left(\frac{1}{K_{VS}} + \frac{1}{K_b}\right) + K_{TF}\right] \quad (5)$$

$$K_{Bolts} = K_{ABB} + K_{TB} \quad (6)$$

where K_{TF} is the flexural stiffness of the steel tube face, K_b is the axial stiffness of the effective embedded length of the bolt, and K_{VS} is the stiffness of the concrete strut. Each of the mentioned stiffnesses can be calculated using the equations presented in Agheshlui *et al*. (2015).

Using Eq. (5), the axial stiffness of the group of four pretensioned bolts without the through bolt was estimated to be 1036 kN/mm. Hence, using Eq. (6), the stiffness of a group of four anchored blind bolts and a through bolt was approximately 1190 kN/mm.

The component model under positive moments is shown in Fig. 19. The four components of the T-stub connection were in series since they were under the same amount of load. They are combined using Eq. (7) which resulted in a translational secant stiffness of 320 kN/mm. The rotational stiffness of the connection was estimated using Eq. (8) assuming that the compression stiffness of the top connection provided by bearing of the T-stub and the slab on the column face was infinitely large compared to the tensile stiffness of the bottom T-stub connection.

$$K_{T-stub} = 1/\left(\frac{1}{K_{T-flange}} + \frac{1}{K_{TS-A}} + \frac{1}{K_{TS-A}} + \frac{1}{K_{Bolts}}\right) \quad (7)$$

$$S = K_{T-stub}\,{Z^+}^2 \quad (8)$$

In Eq. (8) S is the rotational secant stiffness of the composite connection and Z^+ is the lever arm extending from the mid-thickness of the bottom T-stub to two-thirds of the height of the slab (Fig. 19). The rotational stiffness is estimated to be 101,500 kNm/rad which is in good agreement with the stiffness obtained from the test (110,000 kNm/rad). For the composite top connection, the contribution of the slab reinforcement in the connection stiffness needed to be considered. To provide a reasonable estimation of the stiffness of the reinforcement, the bending moment diagram of beams adjacent to a sample connection was considered in the model building. The bending moment diagram under a uniformly distributed gravity load was

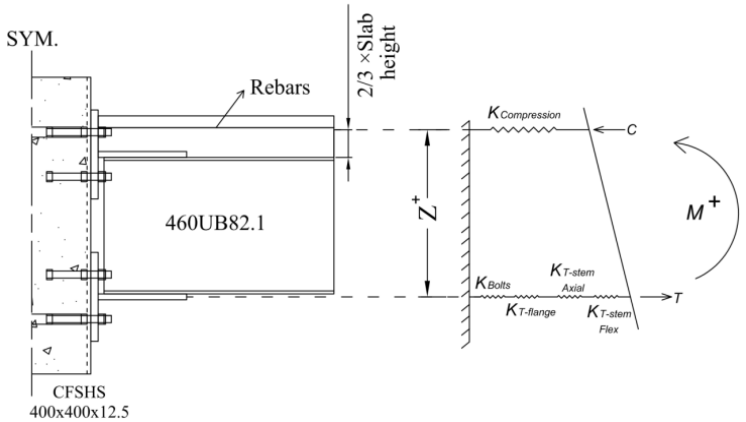

Fig. 19 Component model for the T-stub connection under a positive moment

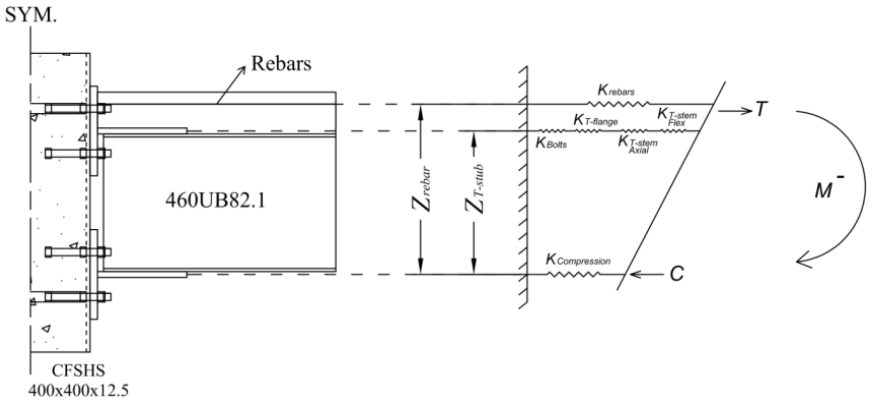

Fig. 20 Component model for the T-stub-Slab connection under a negative moment

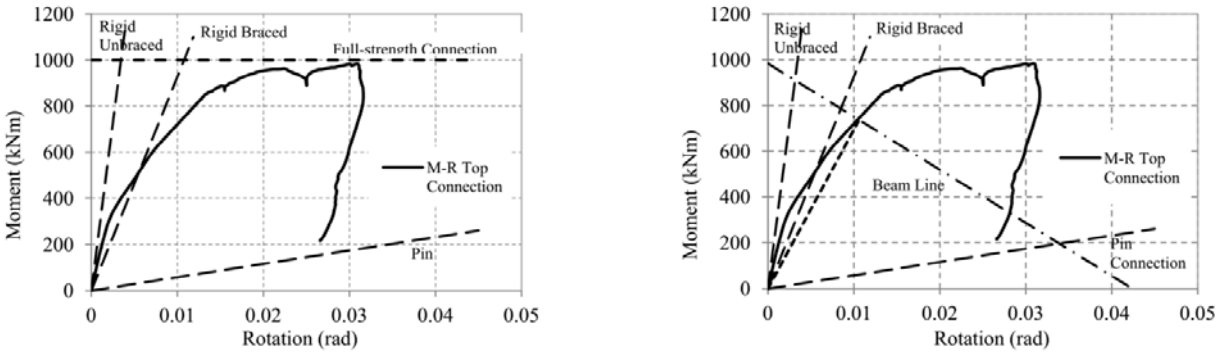

Fig. 21 Connection classification using (a) Eurocode 3 (Eurocode 3 2005); (b) beam-line method

quadratic with zero bending moments at approximately 0.2L away from the connections, where L is the beam span. The bending moment within 0.2L from a connection was negative which applied tension to the reinforcement. For simplicity, the bending moment and the tension produced in the reinforcement were assumed to be linear in this region. The 0.2L was the length of the reinforcement working in tension under the gravity loads and it contributed to the stiffness of the connection. Hence, the stiffness of the reinforcement was calculated using Eq. (9).

$$K_{rebar} = E_s A_s / \left(\frac{L_{rebar}}{2}\right) \tag{9}$$

Where E_s is the elastic modulus of the reinforcement, A_s is the area of the continuous reinforcement, and L_{rebar} is the length of the reinforcement in tension, assumed as 0.2×clear length of span measured face to face of supporting columns. The reinforcement stiffness was divided by 2 to consider the influence of linearly decreasing tension load when moving away from the column.

When lateral loads are applied, the moment diagram of the beams changes and the zero bending moments shift toward or away from the column centreline, depending on the lateral load direction. Consequently, the length of the reinforcement in tension and its stiffness change. In low seismicity areas, the gravity moments are normally large compared to the design earthquake moments. Moreover, the stiffness was higher on one side of the connection and lower on the other side. Hence, it is reasonable to use the average stiffness of the reinforcement on two sides of the connection, considering a reinforcement length of 0.2L, for estimation of the stiffness for such connections within the serviceability limits. Using Eq. (9), the axial stiffness of each rebar was calculated to be 84.8 kN/mm. The rotational stiffness of the connection was estimated using the component model shown in Fig. 20 and Eq. (10) where Z_{rebar} was the distance between the reinforcement and the mid-thickness of the bottom T-stem and $Z_{T\text{-}stub}$ was the distance between the mid-thickness of the T-stubs. The rotational stiffness of the T-stub-Slab connection was found to be 180,000 kNm/rad which was in good agreement with the test result (196,000 kNm/rad).

$$S = K_{T-stub} Z_{T-stub}^2 + K_{rebar} Z_{rebar}^2 \tag{10}$$

4.5.3 Classification of the anchored blind bolted connection

Two methods have been used to classify the proposed connection; the method presented in Eurocode 3 (EN 1993-1-8 2005) and the beam-line method (Reyes-Salazar and Haldar 1999). These classification methods have been originally developed for steel connections. However, in the absence of a classification method for composite joints, the classification method for steel joints has been employed. The connections are thus assumed to be T-stub bolted connections between SHS columns and open section steel beams. In EN 1993-1-8 (2005) classification, the stiffness

of the connection is categorized based on its initial rotational stiffness, $S_{j,ini}$, in comparison with the flexural stiffness of the beam connected to it (EI_b). The connection is rigid if $S_{j,ini} \geq k_b EI_b / L_b$; where, L_b is the span of a beam (centre to centre of columns); $k_b = 8$ for frames in which the bracing system reduces the horizontal displacement by at least 80% (braced frames); and $k_b = 25$ for other frames (unbraced frames) provided that in every storey $k_b / k_c \geq 0.1$ (for frames where $k_b / k_c < 0.1$, the joints should be classified as semi-rigid). The connection would be pinned if $S_{j,ini} \leq 0.5 EI_b / L_b$ (EN 1993-1-8 2005). All the connections for which the stiffness falls between these two boundaries are recognized as semi-rigid connections.

The stiffness of the proposed connection was compared to the stiffness of composite beams connected to it. Composite beams have a significantly higher stiffness compared to I-Beams. Hence, if the beams were made of bare steel, the connection classification would be different. Fig. 21(a) illustrates the classification of the composite anchored blind bolted connection based on EN 1993-1-8 (2005). The connection was categorized as rigid for braced frames and semi-rigid for unbraced frames. The connection stiffness at 2/3 of the design moment was 196,000 kNm/rad which is about 17*EI*/*L*, where *EI* is the flexural stiffness of the composite beam section and *L* is the clear span length of the beam connected to the connection. As shown in Fig. 21(a) the connection showed a reasonable ductility; however, the ductility was partly due to the yielding of anchored blind bolts and the through bolts which was not a desirable ductility source and could result in bolt fracture. The design was to provide ductility by the yielding of the T-flanges. If the bolt loads were limited to 60% of their nominal capacity as intended, the connection strength would have been reduced by an approximate factor of two, while the rotation capacity would have been provided by the yielding of the T-flanges.

The other method that was used for the classification of the connection was the beam line theory, shown in Fig. 21(b). The beam line is a line representing the moment-rotation behaviour of the connected beam section when the beam end condition is changing from a pin to rigid under a distributed load. The intersection of the beam line with the moment rotation curve of the connection is used to define the secant stiffness and to determine if the connection is ductile. If the moment-rotation curve of the connection does not intersect the beam line, the connection would not have adequate rotation capacity and is not suitable as a structural connection. Based on this method, the stiffness of the connection is estimated to be less than the estimated value in accordance with EN 1993-1-8 (2005); however, the connection is still categorized as semi-rigid and ductile.

Similar approaches were used to classify the bottom connection (T-stub only) which was categorized as a semi-rigid connection as well.

4.5.4 General behaviour and observations

In general, the sub-assembly specimen performed well under the applied loads. The connection capacity was found to be higher than the estimated values due to the reasons given in Section 4.5.1. During the application of the gravity loads no sign of nonlinear behaviour or damage was observed. Under cyclic displacements, only small cracks were observed on the face of the concrete slab in the connection region. The cracks became wide toward the end of the cyclic loading and during the downward loading of the beams. The cracking of the concrete under negative moments is shown in Fig. 22(a). Under large compressive stresses during the cyclic loading, which occurred due to the combined effect of positive moments and struts developed from the negative moments as illustrated in Fig. 23, concrete started crushing near the column when ±22 mm displacements were applied at beam ends, Fig. 22(b). The bottom T-flanges started yielding toward the end of the cyclic loading of the specimen (Fig. 17). This continued when both beam ends were subsequently loaded upwards. When both beam ends were loaded downwards, the concrete slab was under tension and the cracks became very wide. The top T-flanges started yielding toward the end of this load step. The yielding of the top T-flange occurred at a larger load compared to the bottom T-flange because of the restraining effect of the concrete slab. No yielding was observed on the tube walls in the connection region even under the ultimate loads.

With regard to the ultimate failure modes, at a moment much larger than the intended design moment, the deck of the concrete slab fractured due to the very large tensile strains. Also, local buckling of the steel tube initiated at the base of the column as shown in Fig. 22(c). At this load level, bolts were about to fracture based on the readings of the load cells (Fig. 16), and also the bolt loads calculated based on the connection moments. However, the test was stopped before the fracture of bolts to avoid damage to the

(a) (b) (c)

Fig. 22 (a) Flexural cracking of the concrete slab near the connection; (b) Crushing of concrete in connection region; (c) steel tube buckling at the base under the ultimate load

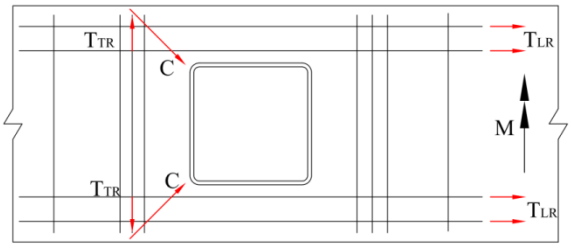

Fig. 23 Strut-tie analogy of the concrete slab near the connection

instrumentation and any other hazard.

5. Simplified method

A simple method for the design of the proposed composite anchored blind bolted connections is provided based on the findings from the sub-assembly test.

5.1 Stiffness of the T-stub connection

The component model for the T-stub connection is illustrated in Fig. 19. The stiffness of the anchored blind bolts can be estimated using equations presented in Agheshlui (2014). The stiffnesses of the rest of the components are given by Eqs. (1) to (3). The stiffness of the compression side of the connection is assumed to be infinite compared to the stiffness of the other components. The translational stiffness and rotational stiffness of the T-stub connection can be calculated using Eqs. (7) and (8), respectively.

(A) Stiffness of the T-stub-Slab connection: The component model for the composite connection of T-stub-Slab is illustrated in Fig. 20. The stiffness of all the components shown in the component model has been already provided. The stiffness of the compression side of the connection is assumed to be infinite compared to the other stiffnesses. The rotational stiffness of the connection can be estimated using Eq. (10).

(B) Yield moment of the T-stub connection: This is recommended to be limited to 60% of the capacity of the bolt group used to connect the T-flange to the CFSHS column. Hence, the yield moment of the T-stub connection can be calculated using Eq. (11).

$$M = 0.6 \times F_{G-ABB} \times Z^{+}_{T-stub} \tag{11}$$

where $F_{G\text{-}ABB}$ is the tensile capacity of the bolt group which is the arithmetic summation of the capacity of all the bolts used for connecting the T-stub to the column. To make sure that the T-stub will yield at around 60% of the capacity of the bolts, the thickness of the T-flange should be limited to the thickness given by Eq. (12)

$$t_{tf} = \left(\frac{2 \times F_{TS} \times m'}{b_{eff}\ F_{y-tf}}\right)^{0.5} \tag{12}$$

Where F_{TS} is the load taken by the T-stub due to $M_{T\text{-}stub}$; $F_{y\text{-}tf}$ is the yield stress of the T-flange; b_{eff} is the effective width of the T-flange and m' is defined in Fig. 18.

(C) Yield moment of the T-stub-Slab connection: Eq. (13) estimates the yield moment of the composite T-stub-Slab connection when the bolt loads are limited to 60% of their capacity. It is assumed that the reinforcement yields when the T-stub starts yielding. This is reasonable due to the large strains occurring in the slab at this stage.

$$M_{T-stub_{Slab}} = 0.6 \times F_{G-ABB} \times Z_{T-stub} + A_s \times F_s \times Z_{rebar} \tag{13}$$

where F_s is the yield stress of the rebars. Eq. (13) can also be used to determine the amount of reinforcement required in the slab by setting the moment capacity equal to the design moment. The area of the required transverse bars near the column is calculated using Eq. (14), based on the strut-tie analogy shown in Fig. 23.

$$A = A_s \times \tan\theta \tag{14}$$

Where A_{tr} is the area of the transverse bars, A_s is the area of the longitudinal bars, and θ is the angle between the concrete strut and the longitudinal rebars ($\approx 45°$). In deriving Eq. (14), it is also assumed that the transverse bars and longitudinal bars have the same yield stress.

6. Conclusions

The use of concrete filled steel tubular columns is not currently popular because of some practical and contractual issues. If these are to be used more extensively, practical, efficient, and reliable bolted connections between these members and open section steel beams need to be developed and tested.

In this project, a new type of blind bolt, the Ajax anchored blind bolt, which was developed (Yao *et al.* 2011) and studied before (Agheshlui 2014), was used to create moment resisting connections between open section steel beams and concrete filled tubular columns. A model building using CFSHS columns, composite beams, and composite connections was designed. The proposed composite connection was made up of double T-stub anchored blind bolted connections which were acting compositely with the reinforced concrete slab. Through bolts were also used in some bolt lines to achieve higher strength.

One sub-assembly from the model building was selected to be tested in full-scale to investigate the behaviour of the composite structural system using anchored blind bolted connections under the gravity and lateral loads of the governing load case. The test showed that the proposed connection, composite with the floor slab, has a high stiffness and capacity. Although the connection was

connected to relatively strong composite beams (steel beam and floor slab), the connection could be categorised as a semi-rigid connection based on Eurocode 3 (EN 1993-1-8 2005) with an stiffness of 17*EI*/*L* for negative bending, where *EI* is the flexural stiffness of the composite beam section and *L* is the clear span length of the beam connected to the connection. The experiment showed that pre-tensioning the bolts connected to the T-flanges applied a clamping force at the bolt lines which resulted in double curvature behaviour of the T-stubs. This provided an increased strength and stiffness for the connections.

The composite action of the floor slab with the connections had a significant influence on the strength and stiffness of the composite connection. The lever arm for a positive connection moment was from the mid-thickness of the bottom T-stem to 2/3 of the height of the floor slab. Interestingly, the behaviour of the anchored blind bolts did not show a significant deterioration due to 21 cycles of loading.

A plastic hinge needed to develop in the connection to avoid overloading the bolts which could result in a relatively non-ductile failure. In this test, the yielding of the T-flanges was selected to provide the plastic rotation capacity.

It was concluded that the proposed connection and system is a viable option to be used in connections to CFSHS columns. For the commercial medium-rise model building, located in a low to medium seismicity region, it was possible to develop a structural lateral force resisting system using blind bolted connections in a way that supplementary systems such as structural walls or bracings were not needed.

A simplified model was presented to approximately represent the behaviour of the specimen. The model estimations were in good agreement with the experimental results obtained here. This model could be used as an estimate of the behaviour of similar bolted connections or as a guide in the design of frames using anchored blind bolted connections. Further experimental and numerical studies are required for expanding the usability of the simplified model and the proposed connection. In particular, the rotation capacity of such connections and the influence of using different material grades need to be investigated.

Acknowledgments

This research program is a part of a research project supported by Australian Research Council, Ajax Engineered Fasteners, and Orrcon Steel through Linkage Project No. LP110200511. The generous contributions of these three research and industry partners are greatly appreciated. The authors also wish to thank Mr. Robert Marshal, Mr. Mitchell Quirk and Mr. Murray Bolden for their great assistance in conducting the test.

References

Agheshlui, H. (2014), "Anchored blind bolted connections within concrete filled square steel hollow sections", The University of Melbourne, Australia.

Agheshlui, H., Goldsworthy, H., Gad, E. and Yao, H. (2015), "Tensile behavior of groups of anchored blind bolts within concrete-filled steel square hollow sections", *J. Struct. Eng.*. **142**(2), 04015125.

Agheshlui, H., Goldsworthy, H., Gad, E. and Fernando, S. (2016), "Tensile behaviour of anchored blind bolts in concrete filled square hollow sections", *Mater. Struct.*, **49**(4), 1511-1525.

AS 1170.2 (2011), Structural design actions - Part 2: Wind actions, Standards Australia.

AS 1170.4 (2007), Structural design actions, Part 4: Earthquake actions in Australia, Standards Australia.

AS 4100 (1998), Australian Standard- Steel structures, Standards Australia.

AS 4291.1 (2000), Mechanical properties of fasteners made of carbon steel and alloys, Part 1: Bolts, screws and studs, Standards Australia.

AS/NZS 1170.0 (2002), Structural design actions, Part 0: General principles, Australian/New Zealand Standard.

AS/NZS 4671 (2001), Australian reinforcing materials, Australian/ New Zealand Standard.

Aslani, F., Uy, B., Tao, Z. and Mashiri, F. (2015), "Predicting the axial load capacity of high-strength concrete filled steel tubular columns", *Steel Compos. Struct., Int. J.*, **19**(4), 967-993.

Bergmann, R., Matsui, C., Meinsma, C. and Dutta, D. (1995), Design guide for concrete filled hollow section columns under static and seismic loading; Verlag TÜV Rheinland, Köln, Germany, CIDECT.

Chung, K.-S., Kim, J.-H. and Yoo, J.-H. (2013), "Experimental and analytical investigation of high-strength concrete-filled steel tube square columns subjected to flexural loading", *Steel Compos. Struct., Int. J.*, **14**(2), 133-153.

EN 1993-1-8 (2005), *D*esign of steel structures, Part 1-8: Design of joints; European Committee for Standardisation (CEN), Brussels, Belgium.

EN 1994-1-1 (2004), Eurocode 4: Design of composite steel and concrete structures. Part 1-1: General rules and rules for buildings, CEN.

Eurocode 3 (2005), Design of steel structures, Part 1-8: Design of joints, European Committee for Standardisation (CEN), Brussels, Belgium.

Faella, C., Piluso, V. and Rizzano, G. (1998), "Experimental analysis of bolted connections: Snug versus preloaded bolts", *J. Struct. Eng.*, **124**(7), 765-774.

FEMA 461 (2007), Interim Testing Protocols for Determining the Seismic Performance Characteristics of Structural and Nonstructural Components.

France, J.E., Buick Davison, J. and A. Kirby, P. (1999), "Moment-capacity and rotational stiffness of endplate connections to concrete-filled tubular columns with flowdrilled connectors", *J. Construct. Steel Res.*, **50**(1), 35-48.

Gardner, A.P. and Goldsworthy, H.M. (2005), "Experimental investigation of the stiffness of critical components in a moment-resisting composite connection", *J. Construct. Steel Res.*, **61**(5), 709-726.

HAZUS MR4 (2003), Multi-hazard Loss Estimation Methodology - Earthquake Model.

Hibbeler, R. (2008), *Mechanics of Materials*, Prentice Hall.

Hicks, S. and Newman, G. (2002), *Design Guide for Concrete Filled Columns*, Corus Tubes.

Lam, N. and Wilson, J. (2004), "Displacement modelling of intraplate earthquakes", *ISET J. Earthq. Technol.*, **41**(1), 15-52.

Liu, Y., Malaga-Chuquitaype, C. and Elghazouli, A.Y. (2014), "Behaviour of open beam-to-tubular column angle connections under combined loading conditions", *Steel Compos. Struct., Int. J.*, **16**(2), 157-185.

Loh, H.Y., Uy, B. and Bradford, M.A. (2006), "The effects of partial shear connection in composite flush end plate joints Part

I — Experimental study", *J. Construct. Steel Res.*, **62**(4), 378-390.
Pitrakkos, T. and Tizani, W. (2015), "A component method model for blind-bolts with headed anchors in tension", *Steel Compos. Struct., Int. J.*, **18**(5), 1305-1330.
Qu, X., Chen, Z. and Sun, G. (2015), "Axial behaviour of rectangular concrete-filled cold-formed steel tubular columns with different loading methods", *Steel Compos. Struct., Int. J.*, **18**(1), 71-90.
Reyes-Salazar, A. and Haldar, A. (1999), "Nonlinear seismic response of steel structures with semi-rigid and composite connections", *J. Construct. Steel Res.*, **51**(1), 37-59.
Ricles, J., Peng, S. and Lu, L. (2004), "Seismic behavior of composite concrete filled steel tube column-wide flange beam moment connections", *J. Struct. Eng.*, **130**(2), 223-232.
Sayers, C.M., Nagy, Z., Adachi, J., Singh, V., Tagbor, K. and Hooyman, P. (2009), *Determination of In-situ Stress and Rock Strength using Borehole Acoustic Data*, Houston, TX, USA.
SCI P213 (1998), *The Steel Construction Institute, Joints in Steel Construction - Composite Connections*.
Tizani, W. and Ridley-Ellis, D. (2003), "The performance of a new blind-bolt for moment-resisting connections", *Proceedings of the 10th International Symposium on Tubular Structures*, Madrid, Spain, September.
Tizani, W., Al-Mughairi, A., Owen, J.S. and Pitrakkos, T. (2013a), "Rotational stiffness of a blind-bolted connection to concrete-filled tubes using modified Hollo-bolt", *J. Construct. Steel Res.*, **80**, 317-331.
Tizani, W., Wang, Z.Y. and Hajirasouliha, I. (2013b), "Hysteretic performance of a new blind bolted connection to concrete filled columns under cyclic loading: An experimental investigation", *Eng. Struct.*, **46**, 535-546.
Wang, J.-F., Han, L.-H. and Uy, B. (2009), "Behaviour of flush end plate joints to concrete-filled steel tubular columns", *J. Construct. Steel Res.*, **65**(4), 925-939.
Yao, H., Goldsworthy, H. and Gad, E. (2008), "Experimental and numerical investigation of the tensile behavior of blind-bolted T-stub connections to concrete-filled circular columns", *J. Struct. Eng.*, **134**(2), 198-208.
Yao, H., Goldsworthy, H., Gad, E. and Fernando, S. (2011). "Experimental study on modified blind bolts anchored in concrete-filled steel tubular columns", *Australian Earthq. Eng. Soc.*, South Australia, Barossa Valley.

DL